J|A|C|S
ARTICLES
Published on Web 08/30/2002

Interaction between f-Electronic Systems in Dinuclear Lanthanide Complexes with Phthalocyanines

Naoto Ishikawa,* Tomochika Iino, and Youkoh Kaizu*

Contribution from the Department of Chemistry, Tokyo Institute of Technology, O-okayama, Meguro-ku, Tokyo 152-8551, Japan

Received May 31, 2002

Abstract: The first detection and characterization of the interactions between the f-electronic systems in the dinuclear complexes of paramagnetic trivalent Tb, Dy, Ho, Er, Tm, and Yb ions with phthalocyanine ligands are presented. The molar magnetic susceptibilities, χ_m, were measured for PcLnPcLnPc* ([Ln, Ln]; Pc = dianion of phthalocyanine, Pc* = dianion of 2,3,9,10,16,17,23,24-octabutoxyphthalocyanine) and PcLnPcYPc* ([Ln, Y]) in the range from 1.8 K to room temperature. The selective synthetic method previously reported for the heterodinuclear complex [Y, Ln] was used to prepare [Ln, Ln] and [Ln, Y] with a modification on the choice of starting materials. The f−f interaction contributions to the magnetic susceptibility are evaluated as $\Delta\chi_m T = \chi_m([Ln, Ln])T - \chi_m([Ln, Y])T - \chi_m([Y, Ln])T$, where T refers to temperature on the kelvin scale. The homodinuclear complexes having f^8−f^{10}-systems, namely [Tb, Tb], [Dy, Dy], and [Ho, Ho], show positive $\Delta\chi_m T$ values in the 1.8−50 K range, indicating the existence of ferromagnetic interaction between the f-systems. The magnitude of the $\Delta\chi_m T$ increases in the descending order of the number of f-electrons. [Er, Er] gives negative $\Delta\chi_m T$ values in the 1.8−50 K range, showing the antiferromagnetic nature of the f−f interaction. [Tm, Tm] exhibits small and negative $\Delta\chi_m T$ values, which gradually decline in the negative direction as the temperature decreases in the range 13−50 K and sharply rise in the positive direction as the temperature falls from 10 to 1.8 K. [Yb, Yb] has extremely small $\Delta\chi_m T$ values, whose magnitude at 2 K is less than 1% of that of [Tb, Tb]. The ligand field parameters of the ground-state multiplets of the six [Ln, Y] complexes are determined by simultaneous fitting to both the magnetic susceptibility data and paramagnetic shifts of ^{1}H NMR. The theoretical analysis successfully converged by assuming that each ligand field parameter is a function of the number of f-electrons in each ion. Using these parameters as well as the previously obtained corresponding parameters for the [Y, Ln] series, the interactions between the f-systems in [Ln, Ln] are investigated. All the characteristic observations above are satisfactorily reproduced with the assumption that the magnetic dipolar term is the sole source of the f−f interaction.

Introduction

One of the unique properties of the related aromatic macrocyclic pigments, phthalocyanines and porphyrins, is their ability to form multilayered compounds known as "double-decker" and "triple-decker" type complexes with trivalent lanthanide ions.[1−3] These compounds have been viewed as "stacked π-conjugate molecules", and their spectroscopic and electrochemical properties have been studied in terms of $\pi-\pi$ interactions between adjacent ligands.[4−6] With an intention to obtain new properties by combining different component π-systems, the syntheses of mixed ligand triple-decker complexes were reported by several groups.[7−10]

In the perspective of "stacked π-conjugate molecules", the lanthanide ions inserted between the ligands have been treated as "bridges" whose length is determined by the ionic radii regularly varying through the lanthanide series. Although the importance of the role of the f-electrons has been mentioned occasionally,[11,12] attention has rarely been paid to the electronic structures of the f-shells in the lanthanide ions, and there has been no decisive study on the sublevel structure of the ground-state multiplets of the complexes.

The "triple-decker" complexes are composed of three dianionic ligands and two trivalent lanthanide ions. Obviously, these compounds have another face as "dinuclear lanthanide complexes". Studying them from this point of view is very important

* Address correspondence to this author. E-mail: ishikawa@chem.titech.ac.jp.

(1) M'Sadak, M.; Roncali, J.; Garnir, F. *J. Chim. Phys.* **1986**, *83*, 211.
(2) Kasuga, K.; Ando, M.; Morimoto, H.; Isa, M. *Chem. Lett.* **1986** 1095.
(3) Buchler, J. W.; De Cian, A.; Fischer, J.; Kihn-Botulinski, M.; Paulus, H.; Weiss, R. *J. Am. Chem. Soc.* **1986**, *108*, 3652.
(4) Ishikawa, N.; Ohno, O.; Kaizu, Y.; Kobayashi, H. *J. Phys. Chem.* **1992**, *96*, 8832.
(5) Ishikawa, N.; Kaizu, Y. *J. Phys. Chem.* **1996**, *100*, 8722.
(6) Ishikawa, N.; Kaizu, Y. *Chem. Phys. Lett.* **1994**, *228*, 625.
(7) Gross, T.; Chevalier, F.; Lindsey, J. S. *Inorg. Chem.* **2001**, *40*, 4762.
(8) Chabach, D.; De Cian, A.; Fischer, J.; Weiss, R.; El Malouli-Bibout, M. *Angew. Chem., Int. Ed. Engl.* **1996**, *35*, 898.
(9) Chabach, D.; Lachkar, M.; De Cian, A.; Fischer, J.; Weiss, R. *New J. Chem.* **1992**, *16*, 431.
(10) Lau, R. L. C.; Jiang, J.; Ng, D. K. P.; Chan, T.-W. D. *J. Am. Soc. Mass Spectrom.* **1997**, *8*, 161.
(11) Liu, W.; Jiang, J.; Pan, N.; Arnold, D. P. *Inorg. Chim. Acta* **2000**, *310*, 140.
(12) Arnold, D. P.; Jiang, J. *J. Phys. Chem. A* **2001**, *105*, 7533.

10.1021/ja027119n CCC: $22.00

because it provides us an opportunity to study a rare class of compounds containing multiple lanthanide ions.

The purpose of this paper is to report the first detection of the f−f interactions in a series of homodinuclear phthalocyanine complexes of Tb^{3+}, Dy^{3+}, Ho^{3+}, Er^{3+}, Tm^{3+}, and Yb^{3+} and the theoretical elucidation of their origin. The two ions are placed along the molecular symmetry axis, and each resides on a ligand field of C_4 symmetry. In X-ray studies on analogous dinuclear cerium complexes with related ligands, the distance between two Ce^{3+} atoms has been reported to be 3.752 Å for $Ce_2(OEP)_3$,[3] 3.84 Å for (TPP)Ce(Pc(OMe)$_8$)Ce(TPP), and 3.66 Å for (Pc)Ce(T(*p*-MeOP)P)Ce(Pc).[9,13] The intermetallic separations are expected to be shorter in the complexes with trivalent lanthanide ions other than the Ce complexes because of the lanthanide contraction. It is naturally anticipated that there would be sizable interactions between the two f-shells, referred to as "f−f interactions" hereinafter, at such short distances.

The detections of f−f interactions have been reported thus far on gadolinium(III) complexes with polydentate ligands such as salicylic acid,[14] 3-methoxysalicylaldehyde,[15] and Schiff bases.[16] In these studies, variations of the effective magnetic dipole moment observed at low temperature are directly assigned to f−f interactions. This assignment is based on an assumption that each individual gadolinium ion, which has seven electrons in the half-filled 4f-shell and hence zero orbital angular momentum, gives a temperature-independent effective magnetic dipolar moment. This approach is, however, inadequate in other lanthanide cases, since the effective magnetic dipolar moments of the non-f^7 lanthanide ions are significantly temperature-dependent, owing to the ligand field splitting of ground-state multiplets.

To study f−f interactions in general lanthanide cases, one needs to know beforehand the electronic structure of individual f-shells. As a solution to this problem, we investigated individual f-shells using newly prepared heterodinuclear complexes composed of a diamagnetic Y^{3+} and a paramagnetic trivalent lanthanide ion, PcYPcLnPc* (abbreviated as [Y, Ln] hereinafter; Pc = dianion of phthalocyanine, Pc* = dianion of 2,3,9,10,16,17,23,24-octabutoxyphthalocyanine, Ln = Tb, Dy, Ho, Er, Tm, and Yb).[17] Through theoretical analysis of the paramagnetic shifts of the ^{1}H NMR spectra and the temperature dependence of the magnetic susceptibilities, we determined ligand field parameters for the six lanthanide cases and elucidated splitting structures of the ground-state multiplets of the heterodinuclear complexes.

Having laid the experimental and theoretical foundation for individual f-systems, we investigate in this paper the f−f interactions in the homodinuclear complexes PcLnPcLnPc* (Figure 1, abbreviated as [Ln, Ln]). By comparison of the temperature dependence of the magnetic susceptibilities between the hetero- and homodinuclear complexes, the net contribution of the f−f interaction terms will be extracted. Similar approaches have been employed to probe d−f interactions in Cu^{2+}−Ln^{3+} compounds:[18,19] the magnetic properties of (Cu^{2+}, Ln^{3+}) pairs were compared with those of isostructural compounds obtained by replacing Cu^{2+} with diamagnetic Zn^{2+} or Ni^{2+}. Each lanthanide system shows a characteristic behavior caused by the f−f interaction, as will be presented. The origin of the f−f interaction in [Ln, Ln] will be discussed using the ligand field parameters determined for [Ln, Y] and [Y, Ln].

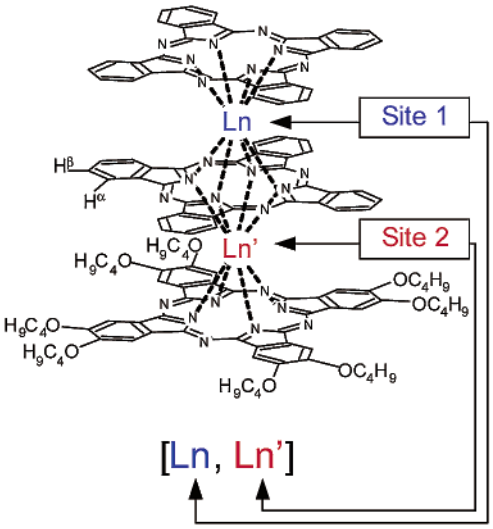

Figure 1. Schematic diagram of PcLnPcYPc(OC$_4$H$_9$)$_8$ ([Ln, Y]; Ln = Tb, Dy, Ho, Er, Tm, and Yb; Ln′ = Y) and PcLnPcLnPc(OC$_4$H$_9$)$_8$ ([Ln, Ln]; Ln = Ln′ = Tb, Dy, Ho, Er, Tm, and Yb).

Experimental Section

General Procedure for the Synthesis of PcLnPcYPc* [Ln, Y] and PcLnPcLnPc* [Ln, Ln] (Ln = Tb, Dy, Ho, Er, Tm, and Yb). The heterodinuclear Pc complexes [Ln, Y] were prepared by the method reported previously for the synthesis of [Y, Ln].[17] Into a 10 mL round-bottom flask equipped with a condensor were placed 20 mg of Pc_2Ln (Ln = Tb, Dy, Ho, Er, Tm, or Yb), 20 mg of H_2Pc*, 80 mg of Y(acac)$_3$·*n*(H_2O), and 5 mL of 1,2,4-triclorobenzene. The mixture was heated in an oil bath set at 60 °C with mechanical stirring until the entire solid was dissolved. The mixture was then refluxed for 3 h, with careful monitoring of the UV spectrum. The reaction solution was cooled to room temperature, and to it was added 80 mL of methanol. The precipitant was filtered, washed with methanol, and extracted with dichloromethane. The extract solution was chromatographed on a silica gel column (Silica Gel 60, Kanto Chemicals, particle size 40−60 μm). Using dichloromethane as eluent, a green band of unreacted Pc_2Ln was initially eluted. The second blue-green band of the target substance was collected. The solution was concentrated, mixed with methanol, and filtered. The chromatographic separation was repeated until the band of unreacted Pc_2Ln disappeared. The final product [Ln, Y] was obtained as a blue-black powder (typically 25 mg). The powder was recrystallized from CH_2Cl_2/hexane. The compounds were identified by elemental analysis and ^{1}H NMR spectroscopy.

Anal. Calcd for $C_{128}H_{112}N_{24}O_8TbY$ ([Tb, Y]): C,65.08; H, 4.78; N, 14.23. Found: C, 65.28; H, 4.90; N, 14.14. Calcd for $C_{128}H_{112}N_{24}O_8$-DyY ([Dy, Y]): C, 64.98; H, 4.77; N, 14.21. Found: C, 64.72; H, 4.90; N, 14.07. Calcd for $C_{128}H_{112}N_{24}O_8HoY$ ([Ho, Y]): C, 64.91; H, 4.76; N, 14.19. Found: C, 65.02; H, 5.00; N, 14.02. Calcd for $C_{128}H_{112}N_{24}O_8ErY$ ([Er, Y]): C, 64.85; H, 4.76; N, 14.18. Found: C, 65.09; H, 4.80; N, 14.12. Calcd for $C_{128}H_{112}N_{24}O_8TmY$ ([Tm, Y]): C, 64.80; H, 4.75; N, 14.17. Found: C, 64.87; H, 4.99; N, 14.00. Calcd

(13) Abbreviation used: OEP, 2,3,7,8,12,13,17,18-octaethylporphyrin dianion; Pc, phthalocyanine dianion; TPP, *meso*-tetra(phenyl)porphyrin dianion; T(*p*-MeOP)P, *meso*-tetra(anisyl)porphyrin dianion; Pc(OMe)8, 2,3,9,10,16,17,-23,24-octamethoxy(phthalocyanine) dianion.
(14) Costes, J.-P.; Clemente-Juan, J. M.; Dahan, F.; Nicodème F.; Verelst M. *Angew. Chem., Int. Ed.* **2002**, *41*, 323.
(15) Costes, J.-P.; Dahan, F.; Nicodème F. *Inorg. Chem.* **2001**, *40*, 5285.
(16) Costes, J.-P.; Dupuis, A.; Laurent J.-P. *Inorg. Chim. Acta* **1998**, *268*, 125.
(17) Ishikawa, N.; Iino, T.; Kaizu, Y. *J. Phys. Chem.*, in press.
(18) Costes, J.-P.; Dahan, F.; Dupuis, A.; Laurent J.-P. *Chem. Eur. J.* **1998**, *4*, 1616.
(19) Kahn, M. L.; Mathonière, C.; Kahn, O. *Inorg. Chem.* **1999**, *38*, 3692.

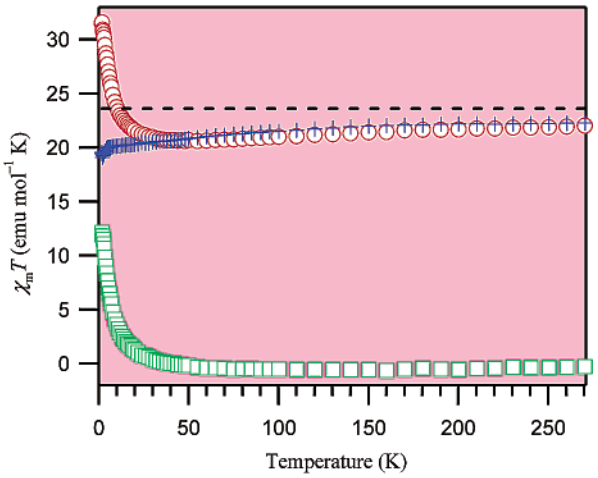

Figure 2. Plots of χ_m([Tb, Tb])T (red circles) and χ_m([Y, Tb])T + χ_m([Tb, Y])T (blue crosses) against temperature T. The difference between the two, $\Delta\chi_m T$, is shown by green squares.

for $C_{128}H_{112}N_{24}O_8YbY$ ([Yb, Y]): C, 64.69; H, 4.75; N, 14.14. Found: C, 64.40; H, 4.98; N, 14.22.

The homodinuclear Pc complexes [Ln, Ln] were obtained by replacing $Y(acac)_3 \cdot n(H_2O)$ with $Ln(acac)_3 \cdot n(H_2O)$ in the method described above for [Ln, Y]. The compounds were identified by elemental analysis and ^{1}H NMR spectroscopy.

Anal. Calcd for $C_{128}H_{112}N_{24}O_8Tb_2$ ([Tb, Tb]: C,63.21; H, 4.64; N, 13.82. Found: C, 63.10; H, 4.69; N, 13.64. Calcd for $C_{128}H_{112}N_{24}O_8Dy_2$ ([Dy, Dy]): C, 63.02; H, 4.63; N, 13.78. Found: C, 63.10; H, 4.70; N, 13.72. Calcd for $C_{128}H_{112}N_{24}O_8Ho_2$ ([Ho, Ho]): C, 62.89; H, 4.61; N, 13.49. Found: C, 62.82; H, 4.89; N, 13.23. Calcd for $C_{128}H_{112}N_{24}O_8Er_2$ ([Er, Er]): C, 62.77; H, 4.60; N, 13.65. Found: C, 62.76; H, 4.88; N, 13.85. Calcd for $C_{128}H_{112}N_{24}O_8Tm_2$ ([Tm, Tm]): C, 62.69; H, 4.60; N, 13.70. Found: C, 62.62; H, 4.43; N, 13.46. Calcd for $C_{128}H_{112}N_{24}O_8Yb_2$ ([Yb, Yb]): C, 62.48; H, 4.58; N, 13.66. Found: C, 62.24; H, 4.57; N, 13.53.

Measurements. Magnetic susceptibility measurements were carried out on a Quantum Design MPMS-5 SQUID (superconducting quantum interference device) magnetometer. To correct for the diamagnetic susceptibility contribution in each the sample, the corresponding experimental data for [Y, Y] were used. ^{1}H NMR spectra of the complexes were measured in $CDCl_3$ solution at 30 °C on a JEOL Lambda-300 NMR spectrometer.

Results

In Figures 2−7, the results the SQUID measurements for [Ln, Ln] are compared with those for [Ln, Y] and [Y, Ln]. The following definition is used hereinafter:

$$\Delta\chi_m T = \chi_m([\mathrm{Ln}, \mathrm{Ln}])T - \{\chi_m([\mathrm{Ln}, \mathrm{Y}])T + \chi_m([\mathrm{Y}, \mathrm{Ln}])T\} \quad (1)$$

where χ_m([Ln, Ln]), χ_m([Ln, Y]), and χ_m([Y, Ln]) refer to the molar magnetic susceptibility of [Ln, Ln], [Ln, Y], and [Y, Ln], respectively, and T is the temperature on the kelvin scale.

[Tb, Tb]. Figure 2 shows the dependence of $\chi_m T$ of [Tb, Tb] on T. As the temperature rises, the $\chi_m T$ value asymptotically approaches that of two free Tm^{3+} ions (2 × 11.81 emu·K/mol). Above 60 K, the difference between χ_m([Tb, Tb])T and χ_m([Tb, Y])T + χ_m([Y, Tb])T is nearly zero. As the temperature falls below 50 K, a steep rise of $\chi_m T$ is seen. The $\Delta\chi_m T$ value reaches 12.0 emu·K/mol at 1.8 K. The positive $\Delta\chi_m T$ values indicate the existence of a ferromagnetic interaction between the Tb ions in [Tb, Tb].

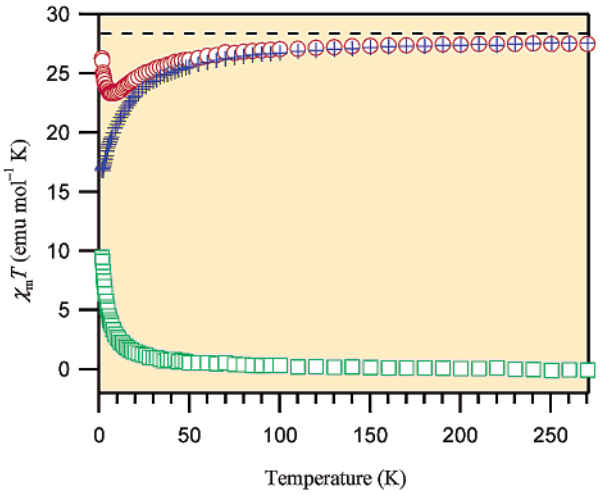

Figure 3. Plots of χ_m([Dy, Dy])T (red circles) and χ_m([Y, Dy])T + χ_m([Dy, Y])T (blue crosses) against temperature T. The difference between the two, $\Delta\chi_m T$, is shown by green squares.

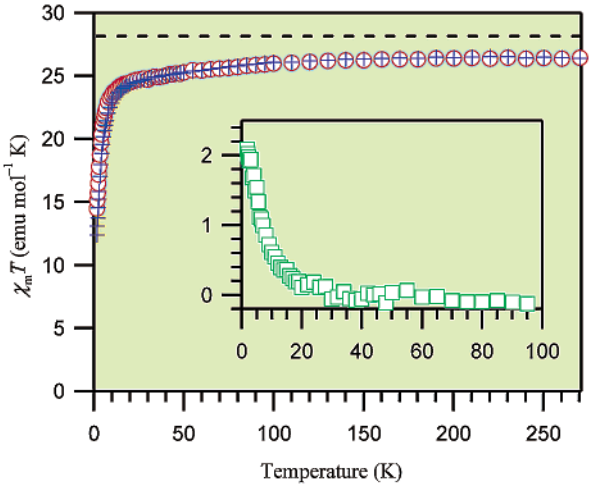

Figure 4. Plots of χ_m([Ho, Ho])T (red circles) and χ_m([Y, Ho])T + χ_m([Ho, Y])T (blue crosses) against temperature T. The difference between the two, $\Delta\chi_m T$, is shown by green squares.

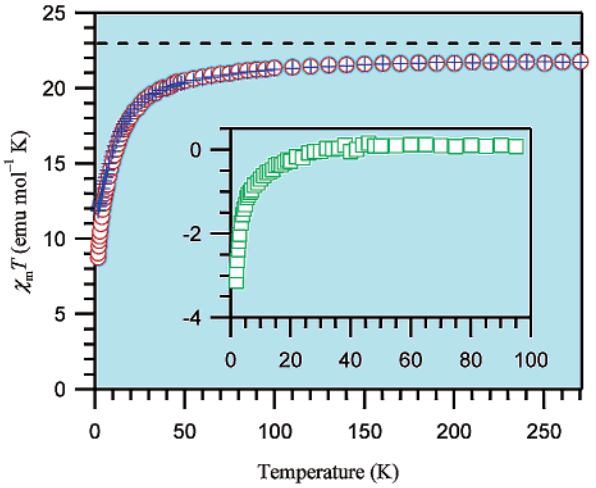

Figure 5. Plots of χ_m([Er, Er])T (red circles) and χ_m([Y, Er])T + χ_m([Er, Y])T (blue crosses) against temperature T. The difference between the two, $\Delta\chi_m T$, is shown by green squares.

[Dy, Dy]. The Dy case exhibits a similar behavior in its $\Delta\chi_m T$ vs T plot (Figure 3). The $\chi_m T$ curve of [Dy, Dy] overlaps the

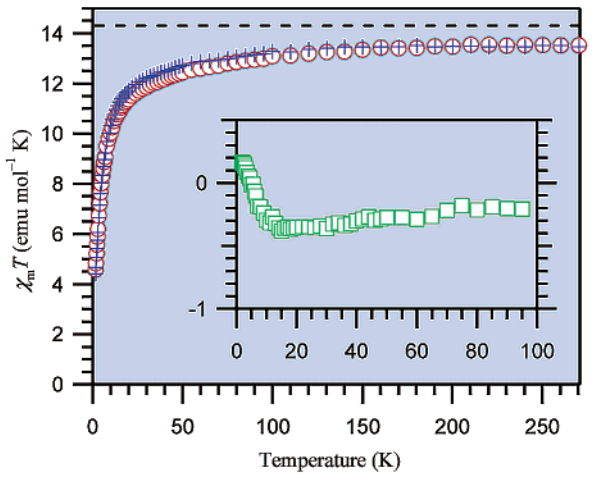

Figure 6. Plots of χ_m([Tm, Tm])T (red circles) and χ_m([Y, Tm])T + χ_m([Tm, Y])T (blue crosses) against temperature T. The difference between the two, $\Delta\chi_m T$, is shown by green squares.

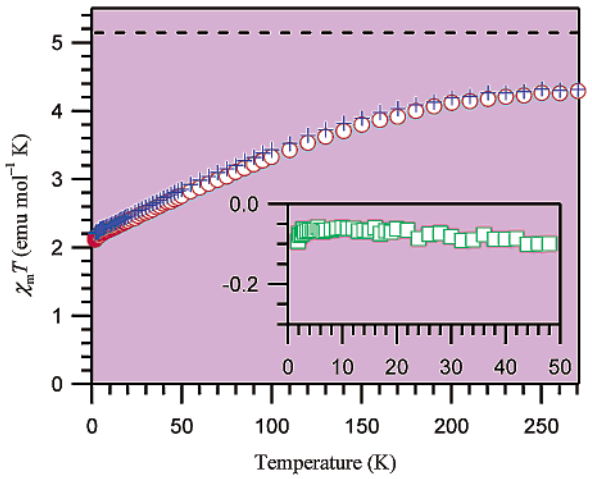

Figure 7. Plots of χ_m([Yb, Yb])T (red circles) and χ_m([Y, Yb])T + χ_m([Yb, Y])T (blue crosses) against temperature T. The difference between the two, $\Delta\chi_m T$, is shown by green squares.

sum of those of [Dy, Y] and [Y, Dy] above 100 K: both approach the $\chi_m T$ value of two free Dy^{3+} ions (2 × 14.18 emu·K/mol). While the ligand-field-only systems, [Dy, Y] and [Y, Dy], show a monotonic decrease in $\chi_m T$ as the temperature drops, $\chi_m T$ of [Dy, Dy] increases after reaching the minimum value at 8 K. A ferromagnetic interaction is expected to exist between the Dy ions in [Dy, Dy].

[Ho, Ho]. The interaction between Ho ions appears ferromagnetic as well, but its magnitude is much smaller than those in the two cases above. As seen in Figure 4, no significant difference is detected between χ_m([Ho, Ho])T and χ_m([Ho, Y])T + χ_m([Y, Ho])T above 30 K. The difference begins to appear below 30 K and increases as the temperature falls. The $\Delta\chi_m T$ value at 1.8 K is about one-sixth of that of [Tb, Tb] and one-fifth of that of [Dy, Dy].

[Er, Er]. The Er case exhibits behavior different than those of the above three cases (Figure 5). Whereas no significant difference is seen between χ_m([Er, Er])T and χ_m([Er, Y])T + χ_m([Y, Er])T above 40 K, $\Delta\chi_m T$ takes a negative value below 40 K, and its magnitude increases as the temperature falls. $\Delta\chi_m T$ reaches −3.1 emu·K/mol at 1.8 K. This indicates that an antiferromagnetic interaction exists between Er ions in [Er, Er].

[Tm, Tm]. The $\Delta\chi_m T$ vs T plot of [Tm, Tm] shows a characteristic pattern in the low-temperature range (Figure 6). The $\Delta\chi_m T$ plot gradually declines in the negative direction as the temperature falls and reaches the negative extreme value at about 13 K. The plot then rapidly rises as T falls from 10 to 1.8 K. The magnitudes of the observed $\Delta\chi_m T$ values are less than 0.4 emu·K/mol throughout the measured temperature. Although the rapid change is small in magnitude, it is not an artifact, as will become clear in the Discussion section later.

[Yb, Yb]. Throughout the temperature region measured, the magnitude of $\Delta\chi_m T$ is less than 0.1 emu·K/mol, which is near the experimental uncertainty level (Figure 7). The interaction between the two f-systems in [Yb, Yb] is apparently the smallest among the six homodinuclear complexes. A small yet detectable decrease in the $\Delta\chi_m T$ value is observed in the region from 3 to 1.8 K.

As already seen in the Tb and Dy systems, there is a common observation in the six cases: the χ_m([Ln, Ln])T values asymptotically approach those of two free Ln^{3+} ions (2 × 14.07 emu·K/mol in [Ho, Ho], 2 × 5.96 emu·K/mol in [Er, Er], 2 × 3.20 emu·K/mol in [Tm, Tm], and 2 × 1.08 emu·K/mol in [Yb, Yb]) as the temperature rises.

Discussion

From the experimental results, the following questions are posed. (1) Why do ferromagnetic interactions exist in [Tb, Tb], [Dy, Dy], and [Ho, Ho]? (2) Why does the interaction becomes antiferromagnetic in [Er, Er]? (3) Is the characteristic behavior of [Tm, Tm] seen in the low-temperature region an artifact or not? (4) Why is the f−f interaction very small in [Yb, Yb]? (5) What is the origin of the f−f interactions in the homodinuclear complexes?

Determination of Ligand Field (LF) Parameters in the Dinuclear Complexes. To discuss the f−f interactions, we have to know beforehand the electronic structure of each f-system. In a previous paper,[17] we reported an analysis of the f-electronic structures of the ions placed between Pc and Pc* ("Site 2" in Figure 1) using the [Y, Ln] series, whose magnetic properties are determined solely by LF terms. The method will be briefly described here and then applied to the [Ln, Y] series to determine the f-structure of the ions on the other side ("Site 1" in Figure 1).

The magnetic properties of a paramagnetic lanthanide ion placed in a ligand field are determined by the following Hamiltonian:

$$\hat{H} = \mu_B(\mathbf{L} + 2\mathbf{S})\cdot\mathbf{H} + \mathbf{F} \qquad (2)$$

The first term of the right-hand side is the Zeeman effect. The second term is the LF potential, which is expressed by the operator equivalent.[20] Following the notation of Abragam and Bleany,[21] the LF term belonging to the C_4 point group is written as

$$\mathbf{F} = A_2^0\langle r^2\rangle\alpha\mathbf{O}_2^0 + A_4^0\langle r^4\rangle\beta\mathbf{O}_4^0 + A_4^4\langle r^4\rangle\beta\mathbf{O}_4^4 + A_6^0\langle r^6\rangle\gamma\mathbf{O}_6^0 + A_6^4\langle r^6\rangle\gamma\mathbf{O}_6^4 \qquad (3)$$

The five coefficients $A_k^q\langle r^k\rangle$ are the parameters to be deter-

(20) Stevens, K. W. H. *Proc. Phys. Soc. A* **1952**, *65*, 209.
(21) Abragam, A.; Bleany, B. *Electron Paramagnetic Resonance*; Clarendon Press: Oxford, 1970.

Table 1. LF Parameters Defined in Eq 4 (in cm^{-1}) for "Site 1" (the Present Paper) and "Site 2" (Ref 17)

	Site 1	Site2		Site 1	Site2
a_2^0	252	244	b_4^4	−22.5	−35.5
b_2^0	−18.7	−24.4	a_6^0	21	15
a_4^0	−191	−183	b_6^0	−0.08	−0.06
b_4^0	9.0	7.0	a_6^4	366	296
a_4^4	643	792	b_6^4	−52.0	−30.6

mined. The $\mathbf{O}_k^q$ matrices are polynomials of the total angular momentum matrices $\mathbf{J}^2$, $\mathbf{J}_z$, $\mathbf{J}_-$, and $\mathbf{J}_+$, and their definitions are described in ref 21. The z axis is chosen to coincide with the C_4 axis. The coefficients α, β, and γ are the constants tabulated by Stevens.[20] The simplex minimization method[22] was used to find a set of LF parameters that gives the least-squares fit to a set of experimental data comprised of the $\chi_m T$ vs T plots and the ^{1}H NMR paramagnetic shifts at 303 K. Since the LF parameters are expected to vary fairly regularly from the f^8-system to the f^{13}-system, we employed an assumption that each parameter is expressed as a linear function of the number of f-electrons, n:

$$A_k^q\langle r^k\rangle(n) = a_k^q + b_k^q(n - 10), \quad n = 8, 9, ..., 13 \qquad (4)$$

Table 1 presents the LF parameters obtained by applying this method for the ions on "Site 1" using the experimental data for [Ln, Y] complexes. Figure 8 shows the theoretical values of the paramagnetic shift $\Delta\delta$ of the ^{1}H NMR chemical shift of the protons on the α position of the center Pc (H^α in Figure 1) and the $\Delta\chi_m T$ values obtained with the best-fit LF parameters. The figure indicates that the LF parameters satisfactorily reproduce all the experimental data.

Interaction between Two f-Systems in [Ln, Ln]. Having obtained the LF parameters of the f-systems of both ions in [Ln, Ln], we are now able to discuss the electronic structures of the homodinuclear complexes. The Hamiltonian for [Ln, Ln] under an external magnetic field is

$$\hat{H} = \mu_B(\mathbf{L}_1 + 2\mathbf{S}_1 + \mathbf{L}_2 + 2\mathbf{S}_2)\cdot\mathbf{H} + \mathbf{F}_1 + \mathbf{F}_2 + \mathbf{V}_{12} \quad (5)$$

$\mathbf{L}_1$, $\mathbf{S}_1$, and $\mathbf{F}_1$ are orbital angular momentum, spin angular momentum, and operator equivalent of the LF potential of the f-system on "Site 1", respectively. The corresponding matrices of the f-system on "Site 2" are denoted by $\mathbf{L}_2$, $\mathbf{S}_2$, and $\mathbf{F}_2$. The size of the matrices is $(2J + 1)^2 \times (2J + 1)^2$. The components of $\mathbf{L}_1$, $\mathbf{S}_1$, $\mathbf{L}_2$, and $\mathbf{S}_2$ are constructed by taking the Kronecker product with the identity matrix as follows:

$$\mathbf{L}_{\xi 1} = \mathbf{L}_\xi \otimes \mathbf{1}$$
$$\mathbf{S}_{\xi 1} = \mathbf{S}_\xi \otimes \mathbf{1}$$
$$\mathbf{L}_{\xi 2} = \mathbf{1} \otimes \mathbf{L}_\xi$$
$$\mathbf{S}_{\xi 2} = \mathbf{1} \otimes \mathbf{S}_\xi$$

where ξ denotes x, y, or z. The ligand field terms are constructed

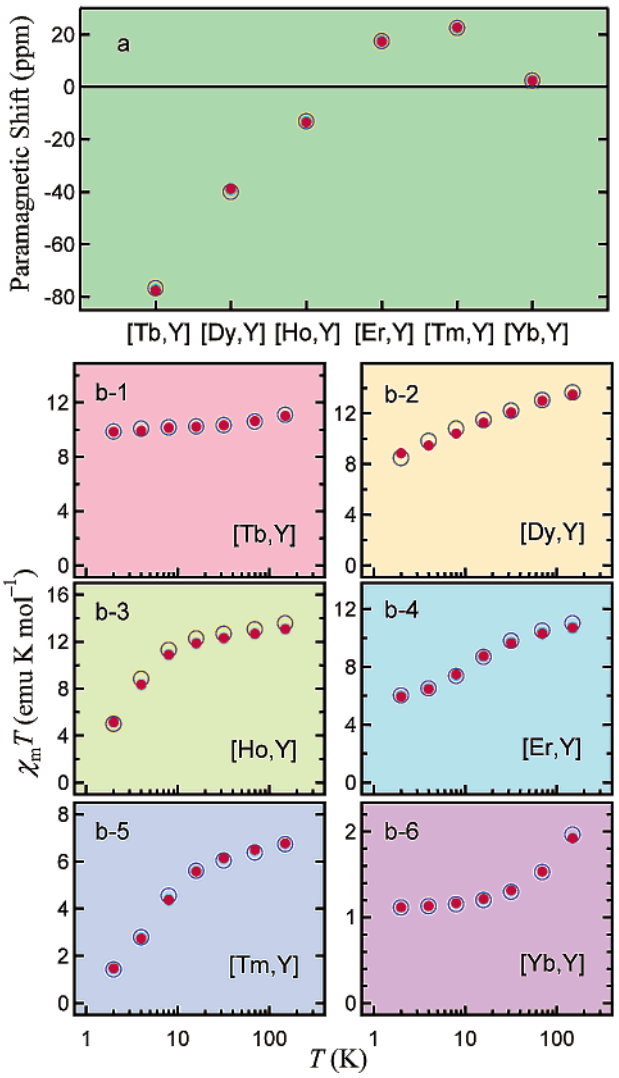

Figure 8. Best-fit result of the simultaneous simulation of (a) paramagnetic shifts of the NMR signal of the proton on the α position of the central Pc ligands in [Ln, Y] (Ln = Tb, Dy, Ho, Er, Tm, and Yb) and (b) temperature dependence of the $\chi_m T$ values of [Ln, Y]. Red closed circles and blue open circles show theoretical and observed values, respectively.

similarly:

$$\mathbf{F}_1 = \mathbf{F}(\text{Site 1}) \otimes \mathbf{1}$$
$$\mathbf{F}_2 = \mathbf{1} \otimes \mathbf{F}(\text{Site 1})$$

where $\mathbf{F}$(Site 1) and $\mathbf{F}$(Site 2) are given by eq 3 with the LF parameters in Table 1. The interaction term $\mathbf{V}_{12}$ is expected to include the exchange contribution and the magnetic dipolar contribution. Inclusion of the former term, $J_{ex}(\mathbf{J}_1\cdot\mathbf{J}_2)$, necessitates introduction of a new parameter, J_{ex}, which cannot be known a priori. On the other hand, the magnetic dipolar term is determined solely by the relative position of the two f-systems, which can be estimated beforehand. We therefore examine the dipolar term first and then estimate how the exchange term contributes. The dipolar term is written as follows:

$$\mathbf{V}_{dip12} = \frac{1}{R^3}\left(\mathbf{M}_1\cdot\mathbf{M}_2 - \frac{3}{R^2}(\mathbf{M}_1\cdot\mathbf{R})(\mathbf{M}_2\cdot\mathbf{R})\right) \qquad (6)$$
$$\mathbf{M}_1 = \mu_B(\mathbf{L}_1 + 2\mathbf{S}_1)$$
$$\mathbf{M}_2 = \mu_B(\mathbf{L}_2 + 2\mathbf{S}_2)$$

(22) Nelder, J. A.; Mead, R. *Computer J.* **1965**, *7*, 308.

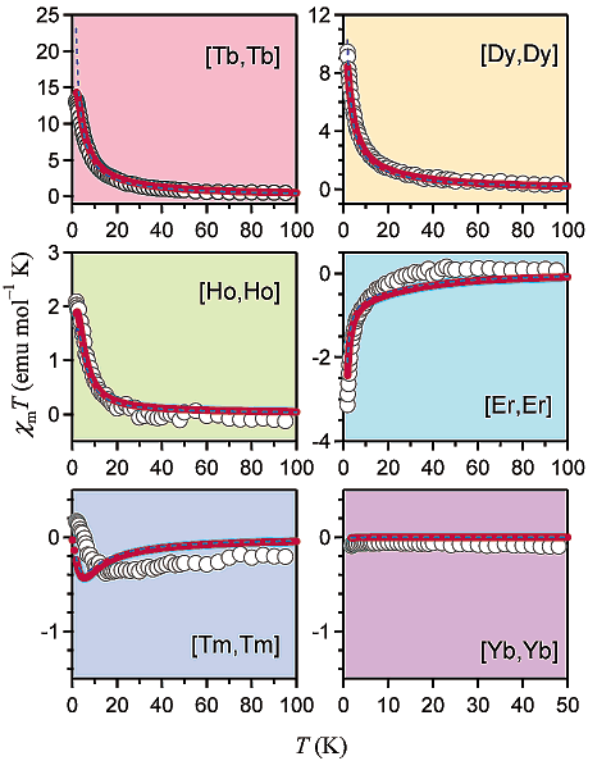

Figure 9. Experimental and theoretical $\Delta\chi_m T$ values of the six lanthanide cases. The experimental data, "full calculation", and "ensemble-averaged approximation" are shown by circles, red solid lines (dotted line below 1.8 K in Ln = Tm), and blue broken lines, respectively.

R is the vector connecting Site 1 and Site 2, and R is the length of **R**. For R, the intermetallic distance obtained by a molecular geometry optimization of Pc_3Y_2 with B3LYP theory[23] was used (R = 3.571 Å). The calculation was performed using the Gaussian 98 program.[24] The basis set employed was LANL2DZ, in which the Los Alamos effective core potential plus double-ζ function[25] is used for the Y atom and Dunning/Huzinaga the full double-ζ function[26] is used for the H, C, and N atoms.

The theoretical values of $\Delta\chi_m T$ obtained from eqs 5 and 6, assuming the presence of the magnetic dipolar interaction, are shown in Figure 9 by solid lines. An overall agreement is seen between the theoretical values and the experimental data of the six [Ln, Ln] systems.

The agreements in the [Tb, Tb], [Dy, Dy], [Ho, Ho], and [Er, Er] cases are quite satisfactory not only in the sign but also in the magnitude of $\Delta\chi_m T$. The theoretical and experimental $\Delta\chi_m T$ values at 1.8K are 14.2 and 12.0 emu·K/mol for [Tb, Tb]; 8.4 and 9.4 emu·K/mol for [Dy, Dy]; 1.9 and 2.1 emu·K/mol for [Ho, Ho]; and −2.4 and −3.1 emu·K/mol for [Er, Er]. Agreements are also seen in the curvature of the $\Delta\chi_m T$ vs T plots.

The diminished magnitude of $\Delta\chi_m T$ of [Tm, Tm] was reproduced in the calculation. More importantly, the model reproduced the rapid rise of the $\Delta\chi_m T$ value observed below 10 K. This indicates that the subtle yet characteristic behavior is not an artifact, but indeed a property of [Tm, Tm]. The model also reproduced the extremely small magnitude of $\Delta\chi_m T$ observed in the [Yb, Yb] case.

The agreement of the model calculation and the experimental data clearly indicates that the interactions between f-electronic systems in the six [Ln, Ln] complexes are essentially of magnetic dipolar nature. The contribution of the exchange interaction term, on the other hand, appears to be very small, if not negligible, compared to that of the dipolar term.

These comparisons, at the same time, can be regarded as a good test of the accuracy of the ligand field parameters determined for [Ln, Y] and [Y, Ln]. The result indicates that the parameters give quite good descriptions of the structure of the f-systems in the present cases.

Let us next discuss how the differences in the $\Delta\chi_m T$ vs T plots among the six cases are caused. To obtain a simplified picture, we carried out calculations of $\Delta\chi_m T$ with a classical view of a magnetic dipole as follows. Each substate of a non-interacting ion on Site 1 or Site 2 is assigned a magnetic susceptibility tensor determined by the LF parameters above. Here, one can assume a model in which each lanthanide ion has an ensemble-averaged molecular magnetic susceptibility tensor, instead of a set of the substate susceptibility tensors. In this model, an external magnetic field H_ξ ($\xi = x, y,$ or z) induces a single magnetic dipole on each lanthanide site. The induced dipole on Site 1 creates a magnetic field $H_{\xi 12}$ on Site 2. As a result, the effective molecular magnetic susceptibility of Site 2 becomes $(1 + H_{\xi 12}/H_\xi)\chi_{\xi 2}$, where $\chi_{\xi 2}$ is for the non-interacting system. Considering the corresponding effect on Site 1, the variations in χ_ξ and the molar magnetic susceptibility are written as

$$\Delta\chi_\xi = -2\frac{\chi_{\xi 1}\chi_{\xi 2}}{R^3}, \quad \xi = x,y \tag{7}$$

$$\Delta\chi_\xi = 4\frac{\chi_{\xi 1}\chi_{\xi 2}}{R^3}, \quad \xi = z \tag{8}$$

$$\Delta\chi_m = \frac{N_A}{3}(\Delta\chi_x + \Delta\chi_y + \Delta\chi_z) \tag{9}$$

where N_A is the Avogadro number.

The results obtained by this "ensemble-averaged approximation" are shown by the broken lines in Figure 9. In each case, the approximation gives a fairly accurate description of the "full" calculation, which takes into account all the substate-to-substate interactions. The model appears to provide a sufficiently meaningful picture of the interaction between the f-systems. Let us next look at the ensemble-averaged magnetic susceptibility tensors of the non-interacting and interacting systems.

Figure 10 illustrates the magnetic susceptibility tensors for the cases of Tb, Dy, and Ho systems at 4 K. The common characteristic of the three systems is that the closed surfaces representing the χ_ξ tensors of [Ln, Y] and [Y, Ln] are both

(23) Becke, A. D. *J. Chem. Phys.* **1993**, *98*, 5648−5652.
(24) Frisch, M. J.; Trucks, G. W.; Schlegel, H. B.; Scuseria, G. E.; Robb, M. A.; Cheeseman, J. R.; Zakrzewski, V. G.; Montgomery, J. A., Jr.; Stratmann, R. E.; Burant, J. C.; Dapprich, S.; Millam, J. M.; Daniels, A. D.; Kudin, K. N.; Strain, M. C.; Farkas, O.; Tomasi, J.; Barone, V.; Cossi, M.; Cammi, R.; Mennucci, B.; Pomelli, C.; Adamo, C.; Clifford, S.; Ochterski, J.; Petersson, G. A.; Ayala, P. Y.; Cui, Q.; Morokuma, K.; Malick, D. K.; Rabuck, A. D.; Raghavachari, K.; Foresman, B.; Cioslowski, J.; Foresman, J. B.; Cioslowski, J.; Ortiz, J. V.; Baboul, A. G.; Stefanov, B. B.; Liu, G.; Liashenko, A.; Piskorz, P.; Komaromi, I.; Gomperts, R.; Martin, R. L.; Fox, D. J.; Keith, T.; Al-Laham, M. A.; Peng, C. Y.; Nanayakkara, A.; Gonzalez, C.; Challacombe, M.; Gill, P. M. W.; Johnson, B. G.; Chen, W.; Wong, M. W.; Andres, J. L.; Head-Gordon, M.; Replogle, E. S.; Pople, J. A. *Gaussian 98*, Revision A.11; Gaussian, Inc.: Pittsburgh, PA, 2001.
(25) (a) Hay, P. J.; Wadt, W. R. *J. Chem. Phys.* **1985**, *82*, 270. (b) Hay, P. J.; Wadt, W. R. *J. Chem. Phys.* **1985**, *82*, 284. (c) Hay, P. J.; Wadt, W. R. *J. Chem. Phys.* **1985**, *82*, 299.
(26) Dunning, T. H., Jr.; Hay, P. J. In *Modern Theoretical Chemistry*; Schaefer, H. F. III, Ed.; Plenum: New York, 1976; pp 1−28.

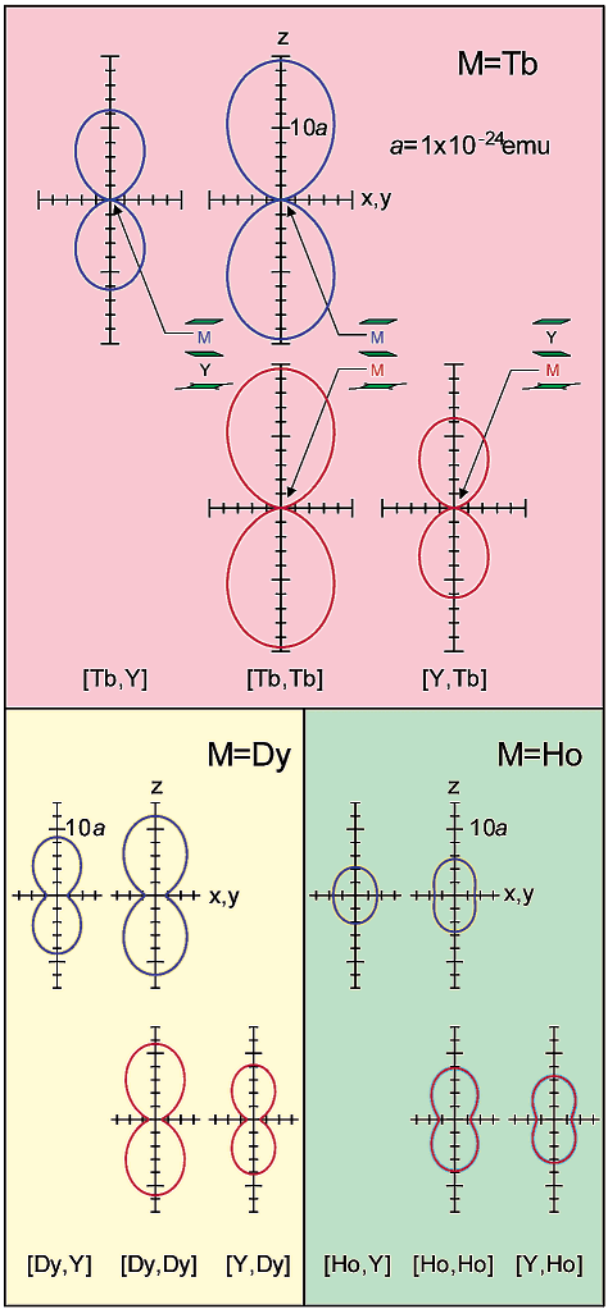

Figure 10. *xz* cross sections of the closed surfaces representing anisotropic magnetic susceptibility tensors of [Y, Ln], [Ln, Ln], and [Ln, Y] (Ln = Tb, Dy, and Ho) at 4 K. Each closed surface is generated by revolving the corresponding closed curve around its *z* axis. A vector from one of the coordinate origins to a point on the surface represents the projection of the induced magnetic dipole on the direction vector of a unit external magnetic field.

longitudinally extending. The height of the closed surfaces of [Ln, Ln] is increased compared to that of the non-interacting systems in the three cases. This is caused by eq 8, whose effect is to increase χ_z in the interacting systems. The net increase $\Delta\chi_m$ takes a positive value because χ_z is greater than χ_x and χ_y, and $\Delta\chi_z$ is dominant in eq 9. The extreme anisotropy in the χ_ξ tensor of the Tb ions explains the largeness of the $\Delta\chi_m T$ value observed in [Tb, Tb]: the positive $\Delta\chi_z$ is largest among the six systems and the negative $\Delta\chi_x$ and $\Delta\chi_y$ are negligible, leading to the maximum $\Delta\chi_m$ value.

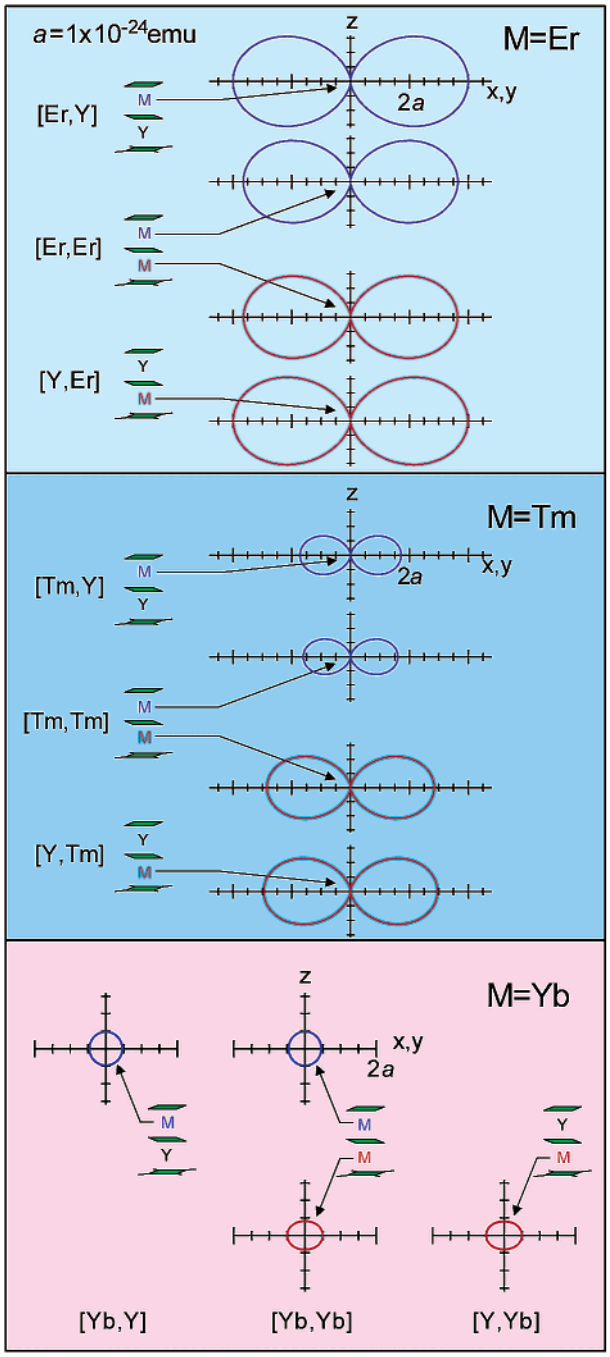

Figure 11. *xz* cross sections of the closed surfaces representing anisotropic magnetic susceptibility tensors of [Y, Ln], [Ln, Ln], and [Ln, Y] (Ln = Er, Tm, and Yb) at 4 K. Each closed surface is generated by revolving the corresponding closed curve around its *z* axis. A vector from one of the coordinate origins to a point on the surface represents the projection of the induced magnetic dipole on the direction vector of a unit external magnetic field.

On the other hand, the closed surfaces for the χ_ξ tensors of [Er, Y] and [Y, Er] are laterally extending, meaning χ_z is smaller than χ_x and χ_y (Figure 11). The horizontal width of the closed surface of [Er, Er] is reduced significantly by eq 7. Since the contribution from the negative $\Delta\chi_x$ and $\Delta\chi_y$ is dominant, $\Delta\chi_m$ is negative in the interacting system. The Tm case is similar picture to the Er case. The smallness of the $\Delta\chi_m T$ values in the Tm case is attributed to the relative smallness of the χ_x and χ_y values compared to those in the Er case.

The closed surfaces for the χ_ξ tensor of [Yb, Y] and [Y, Yb] are close to being spherical, meaning that the magnetic susceptibilities are nearly isotropic. In general, if $\chi_{\xi 1}$ and $\chi_{\xi 2}$ are isotropic, $\Delta\chi_m$ is zero. The extreme diminishment in $\Delta\chi_m T$ values observed in the Yb case is explained by the small anisotropy in magnetic susceptibility in the non-interacting systems.

Conclusions

Comparison of the temperature dependence of magnetic susceptibilities between newly synthesized homo- and heterodinuclear complexes has given a clear insight into the diverse types of f−f interactions in the six lanthanide cases. On the basis of the theoretical calculations using the LF parameters determined for each lanthanide site, we have reached the conclusion that the interaction between the f-systems in [Ln, Ln] (Ln = Tb, Dy, Ho, Er, Tm, Yb) is essentially of magnetic-dipolar nature. The following observations can all be explained by the anisotropy in the magnetic susceptibility of the non-interacting f-systems. (1) The interaction is ferromagnetic in [Tb, Tb], [Dy, Dy], and [Ho, Ho]. (2) The interaction is antiferromagnetic in Er and Tm systems. (3) The $\Delta\chi_m T$ values are extremely small in the Yb system. The method for analysis of f−f interactions described herein is readily applicable to the mixed phthalocyanine−porphyrin triple-decker complexes[7−10] and also the recently emerged classes of dinuclear lanthanide complexes such as "helicates" with polydentate ligands based on benzimidazole and pyridine[27−29] or dipicolinic acid.[30,31] We believe that the present work, together with the previous paper,[17] provides a versatile tool to investigate the electronic structure of a wide range of mono- and dinuclear lanthanide complexes.

Acknowledgment. This work was partially supported by a Grant-in-Aid for Science Research (No. 13740375) from the Ministry of Education, Science, Sports and Culture in Japan. The authors express their gratitude to Prof. Toshiaki Enoki, Dr. Hirohiko Sato, Dr. Akira Miyazaki, and Dr. Kazuyuki Takai at Tokyo Institute of Technology for permission to use the SQUID instrument and invaluable help. Thanks are also due to Prof. Katsumi Kakinuma and Prof. Tadashi Eguchi for permission to use the NMR spectrometer. Last, but not least, we gratefully thank Dr. Ken Ohmori for the invaluable help with the NMR measurements.

JA027119N

(27) Elhabiri, M.; Scopelliti, R.; Bunzli, J.-C. G.; Piguet, C. *J. Am. Chem. Soc.* **1999**, *121*, 10747.
(28) Martin, N.; Bünzli, J.-C. G.; McKee, V.; Piguet, C.; Hopfgartner, G. *Inorg. Chem.* **1998**, *37*, 577.
(29) Muller, G.; Bünzli, J.-C. G.; Schenk, K. J.; Piguet, C.; Hopfgartner, G. *Inorg. Chem.* **2001**, *40*, 2642.
(30) Lessmann, J.; Horrocks, W. D., Jr. *Inorg. Chem.* **2000**, *39*, 3124.
(31) Ouali, N.; Bocquet, B.; Rigault, S.; Morgantini, P.-Y.; Weber, J.; Piguet, C. *Inorg. Chem.* **2002**, *41*, 1436.